SCIENCE CHINA
Chemistry

• ARTICLES •
• SPECIAL TOPIC • Frontiers in Polymer Science

December 2016 Vol.59 No.12: 1583–1592
doi: 10.1007/s11426-016-0203-5

Design, synthesis and photovoltaic properties of a series of new acceptor-pended conjugated polymers

Zhihong Wu, Yongxiang Zhu, Wei Li, Yunping Huang, Junwu Chen, Chunhui Duan*, Fei Huang* & Yong Cao

Institute of Polymer Optoelectronic Materials and Devices, State Key Laboratory of Luminescent Materials and Devices, South China University of Technology, Guangzhou 510640, China

Received May 2, 2016; accepted May 25, 2016; published online October 25, 2016

A series of novel acceptor-pended conjugated polymers featuring a newly developed carbazole-derived unit are designed and synthesized. The relationships between chemical structure and optoelectronic properties of the polymers are systematically investigated. The control of UV-Vis absorption spectra and energy levels in resulting polymers are achieved by introducing suitable pended acceptor units. The photovoltaic properties of the resulting polymers are evaluated by blending the polymers with (6,6)-phenyl-C_{71}-butyric acid methyl ester. The resulting solar cells exhibit moderate performances with high open-circuit voltage. Charge transport properties and morphology were investigated to understand the performance of corresponding solar cells.

acceptor-pended conjugated polymers, polymer solar cells, band gap, energy level

Citation: Wu Z, Zhu Y, Li W, Huang Y, Chen J, Duan C, Huang F, Cao Y. Design, synthesis and photovoltaic properties of a series of new acceptor-pended conjugated polymers. *Sci China Chem*, 2016, 59: 1583−1592, doi: 10.1007/s11426-016-0203-5

1 Introduction

In the past decade, polymer solar cells (PSCs) consist of a phase-separated blend of an electron-donating conjugated polymer and an electron-accepting fullerene derivative have gained enormous attractions due to their unique advantages including low-cost, light weight, mechanical flexibility and their potential for making large area flexible devices [1–6]. Recently, significant progress have been made in improving the performance of PSCs, with power conversion efficiency (PCE) up to 10% has been attained for small-area single junction devices [7–14]. In PSCs, electron-donating conjugated polymers play a crucial role as they harvest the energy of sun light and transport charge carriers. To realize high performance PSCs, it is critical to develop a polymer with an absorption spectrum matching well with solar spectrum, fine-tuned energy levels, and excellent hole transport property at the same time [15–18]. Recent successful examples in developing novel conjugated polymers usually apply donor-acceptor molecular design, since the hybridization of the energy levels of the donor and acceptor can narrow optical band gap and fine-tuned side chains afford the polymer good processability and proper miscibility with fullerene to form optimal morphology [19–20]. Besides the widely studied donor-acceptor polymers with linear backbones, acceptor-pended conjugated polymers also received considerable attentions due to their unique advantages [21]. In this polymer design, the absorption bands and energy levels of the resulting conjugated polymers can be readily tuned by changing the acceptors in the side chain. Furthermore, the two-dimensional like structures may endow the polymers good solubility and desired isotropic charge transporting abilities [22–38].

*Corresponding authors (email: chunhui.duan@gmail.com; msfhuang@scut.edu.cn)

Triphenylamine is one of the most widely used building unit in constructing acceptor-pended conjugated polymers in previous reports owing to their unique merits, such as excellent hole transporting ability, outstanding thermal and oxidation stability, and facile accessibility [22–26,28,31,32, 39]. However, the propeller structure of triphenylamine unit may constraint the conjugate length of along polymer main chain and limit electron delocalization between main chain and pended side chain, which are unfavorable for hole transporting along polymer main chain and electron coupling in the side chain direction. We thus focus on reducing the rotation freedom of propeller-shaped triphenylamine (Scheme 1), aiming at improving hole transporting abilities of the polymers and enhancing photovoltaic property of the final devices.

Herein, we report the design and synthesis a series of novel acceptor-pended conjugated polymers (PFC-DCN, PFC-DTA, PCC-DCN and PCC-DTA) based on a newly developed carbazole-derived moiety. The thermal, optical, and electrochemical properties of the resulting polymers are systematically studied. The photovoltaic properties of the polymers are investigated via blending the polymers with (6,6)-phenyl-C71-butyric acid methyl ester ($PC_{71}BM$). All polymers display moderate photovoltaic performance with the best PCE of 2.0% attained for PCC-DCN.

2 Experimental

2.1 General details

Carbazole, 1,4-dibromobenzene, $POCl_3$ and diethyl (2-methylthiophene)-phosphonate were purchased from Alfa Aesar (USA). Malononitrile, 1,3-diethyl-2-thiobarbituric acid were purchased from Acros (Belgium). $Pd(PPh_3)_4$ was purchased from Sigma-Aldrich (USA). All the reagents were used without further purification. All the solvents used were purified prior to use according to normal procedure. Other materials were common commercial level and used as received. ^1H NMR and ^{13}C NMR spectra were recorded on a Bruker AV-300 (300 MHz) (Germany) in deuterated chloroform solution using tetramethylsilane (TMS; δ=0 ppm) as internal standard. Molecular weight and polydispersity indice (PDI) of the polymers were determined by a Waters GPC 2410 (USA) in tetrahydrofuran (THF) using a calibration curve with standard polystyrene as a reference. Thermogravimetric analyses (TGA) were performed on a Netzsch TG 209 (Germany) under N_2 flow at a heating rate of 10 °C min^{-1}. Differential scan calorimetry (DSC) measurements were performed on a Netzsch DSC 204 (Germany) under N_2 flow at heating and cooling rates of 10 °C min^{-1}. UV-Vis absorption spectra were recorded on a Hewlett Packard (HP) 8453 spectrophotometer (USA). Cyclic voltammetry (CV) was performed on a CHI800C electrochemical workstation (CH Instruments Inc., China) with a platinum working electrode and a Pt wire counter electrode at a scan rate of 50 mV s^{-1} against a saturated calomel electrode (SCE) reference electrode with a nitrogen-saturated anhydrous solution of 0.1 mol L^{-1} tetrabutylammonium hexafluorophosphate in acetonitrile. The polymer films for electrochemical measurements were coated from a polymer-THF dilute solution.

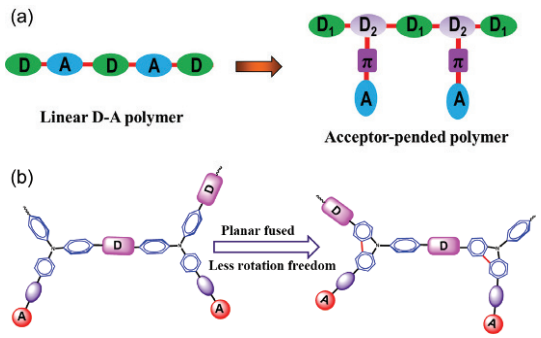

Scheme 1 The illustration of acceptor-pended polymer (a) and our new polymer design (b) (color online).

2.2 Fabrication of hole-only devices

Hole mobility was measured in hole-only devices by using the space charge limited current (SCLC) method with a device configuration of ITO/PEDOT:PSS/active layer/MoO_3/Al. The mobility were determined by fitting the dark current to the model of a single carrier SCLC with field-dependent mobility, which was described by the Mott-Gurney square law: $J=(9/8)\varepsilon_0\varepsilon_r\mu((V^2)/(d^3))$, where J was the current, μ was the zero-field mobility, ε_0 was the permittivity of free space, ε_r was the relative permittivity of the material, d was the thickness of the active layer, and V was the effective voltage.

2.3 Fabrication and characterization of PSCs

A PEDOT:PSS layer (~40 nm) was spun on indium tin oxides (ITO) substrate and dried at 140 °C for 20 min in air, thereafter the blended solution was prepared by mixing copolymer and $PC_{71}BM$ into the mixed solvent (chloroform/chlorobenzene=1:1, *v*/*v*) and subsequent spin coating of the solutions onto the PEDOT:PSS film were carried out in a N_2-filled glove box, followed by annealing at 150 °C for 10 min. Finally, the devices were completed with the deposition of a Ca (10 nm)/Al (100 nm) cathode under high vacuum. The resultant photovoltaic cells were then encapsulated by an UV-curable epoxy resin and tested under ambient conditions using a Keithley Instruments Model 2400 (USA) source-measurement unit and an Oriel xenon lamp (450 W, Enlitech, Taiwan, China) with an AM1.5 filter. The illumination intensity of the light source was calibrated before the testing using a standard silicon solar cell with a KG5 filter, calibrated using a National Renewable Energy Laboratory

(NREL) calibrated silicon photodiode, giving a value of 100 mW cm^{-2} in the test. The current density-voltage (*J-V*) characteristics of the devices were recorded with a Keithley 2400 source meter.

2.4 Synthesis of monomers and polymers

2,7-Bis(4,4,5,5-tetramethyl-1,3,2-dioxaborolan-2-yl)-9,9-dioctylfluorene [40], and 2,7-bis(4,4,5,5-tetramethyl-1,3,2-dioxaborolan-2-yl)-*N*-9-heptadecanylcarbazole [41] were prepared according to the reported procedures.

2.4.1 9-(4-Bromophenyl)-9*H*-carbazole (**C1**)

To a solution of carbazole (1.67 g, 10 mmol) and 1,4-dibromobenzene (4,72 g, 20 mmol) in 2 mL of 1,3-dimethyl-2-oxohexahydropyrimidine (DMPU), 18-crown-6 (100 mg), K_2CO_3 (5.52 g, 40 mmol) and CuI (0.76 g, 4 mmol) were added under nitrogen atmosphere. The reaction mixture was heated to 150 °C and stirred for 12 h under this temperature. After cooling to room temperature, water was added and the mixture was extracted with dichloromethane for three times. The collected organic phases were washed with water and sequentially dried over anhydrous $MgSO_4$. The solvent was removed under reduced pressure and the residue was subjected to silica gel column. The pure product was obtained by eluting the silica gel column with petroleum ether/dichloromethane (5:1, *v*/*v*) as a white solid (0.97 g, 30% yield). ^{1}H NMR ($CDCl_3$, 300 Hz), (ppm): 8.15–8.12 (d, *J*=7.4 Hz, 2H), 7.93–7.90 (d, *J*=8.5 Hz, 0.25 H), 7.74–7.71 (d, *J*=8.5 Hz, 1.75 H), 7.46–7.29 (m, 6H), 7.24 (m, 2H). ^{13}C NMR ($CDCl_3$, 75 Hz), δ (ppm): 140.63, 139.10, 136.83, 133.13, 128.96, 128.74, 126.10, 123.51, 120.91, 120.41, 120.23, 109.56.

2.4.2 9-(4-Bromophenyl)-9*H*-carbazole-3-carbaldehyde (**C2**)

$POCl_3$ (1 mL) was added into 3 mL of *N*,*N*-dimethylformamide (DMF) at 0 °C under nitrogen atmosphere, and the mixture was warmed to room temperature. After stirring for 30 min, the solution of **C1** (1.61 g, 5 mmol) in 1,2-dichloroethane (10 mL) was added into the reaction in one portion. The reaction was heated to refluxing and was stirred for 12 h. After cooling to room temperature, saturated sodium acetate aqueous solution was added. The mixture was extracted with dichloromethane for three times. The organic phases were collected and dried over anhydrous $MgSO_4$. The solvent was removed on rotary evaporator and the residue was subjected to silica gel column and was eluted with petroleum ether/dichloromethane (1:2, *v*/*v*). The titled compound **C2** was obtained as a white solid (1.1 g, 63% yield). ^{1}H NMR ($CDCl_3$, 300 Hz), (ppm): 10.12 (s, 1H), 8.66 (s, 1H), 8.21–8.19 (d, *J*=7.2 Hz, 1H), 7.96–7.94 (d, *J*=8.3 Hz, 1.2H), 7.79–7.76 (d, *J*=8.3 Hz, 1.8H), 7.48–7.29 (m, 5H). ^{13}C NMR ($CDCl_3$, 75 Hz), δ (ppm): 191.65, 144.22, 141.60, 139.40, 135.80, 133.42, 129.71, 128.99, 128.81, 127.63, 127.17, 123.76, 123.34, 122.01, 121.48, 120.78, 110.18, 109.91.

2.4.3 6-Bromo-9-(4-bromophenyl)-9*H*-carbazole-3-carbaldehyde (**C3**)

C2 (1 g, 2.86 mmol) was dissolved in 15 mL of dichloromethane and the solution was cooled to 0 °C. A solution of bromine (457 mg, 2.86 mmol) in 10 mL of dichloromethane was added dropwise under nitrogen atomsphere. After stirring at 0 °C for 5 h, the reaction was warmed to room temperature and 20 mL $NaHSO_3$ aqueous solution was added. The mixture was extracted with dichloromethane and the organic phases were collected. The solvent was removed under reduced pressure and the residue was recrystallized from methanol to afford a white solid (980 mg, 80% yield). ^{1}H NMR ($CDCl_3$, 300 Hz), δ (ppm): 10.10 (s, 1H), 8.58 (s, 1H), 8.29 (s, 1H), 7.98–7.96 (d, *J*=8.4Hz, 1H), 7.79–7.76 (d, *J*=8.5 Hz, 2H), 7.56–7.53 (d, *J*=8.7 Hz, 1H), 7.42–7.39 (d, *J*=8.4 Hz, 3H), 7.24–7.22 (d, *J*=8.7 Hz, 1H). ^{13}C NMR ($CDCl_3$, 75 Hz), δ (ppm): 191.38, 144.39, 140.24, 135.33, 133.56, 130.01, 129.91, 128.79, 128.70, 127.98, 125.04, 124.17, 123.57, 122.60, 122.38, 114.34, 111.67, 110.23.

2.4.4 3-Bromo-9-(4-bromophenyl)-6-(2-(thiophen-2-yl)-vinyl)-9*H*-carbazole (**C4**)

To a solution of **C3** (2.15 g, 5 mmol) and diethyl (2-methylthiophene)-phosphonate (1.4 g, 6 mmol) in 20 mL of dry THF, potassium *tert*-butoxide (0.57 g, 6 mmol) was added at room temperature under nitrogen atmosphere. The solution was changed from light yellowish to brownish-red immediately. The reaction was stirred overnight, and water was added. The reaction was extracted with dichloromethane and the collected organic phases were washed with water and dried over anhydrous $MgSO_4$. The solvent was removed on rotary evaporator and the residue was subjected to silica gel column. After eluting with petroleum/dichloromethane (1:1, *v*/*v*), a pure titled compound **C4** was obtained as a light yellowish solid (2.2 g, 86% yield). ^{1}H NMR ($CDCl_3$, 300 Hz), δ (ppm): 8.20 (s, 1H), 8.07 (s, 1H), 7.71–7.68 (d, *J*=8.3 Hz, 2H), 7.52–7.43 (m, 2H), 7.35–7.32 (d, *J*=8.3 Hz, 2H), 7.23–7.16 (m, 4H), 7.08–7.00 (m, 3H). ^{13}C NMR ($CDCl_3$, 75 Hz), δ (ppm): 143.25, 140.46, 139.65, 136.15, 133.28, 130.03, 128.99, 128.64, 128.45, 127.65, 125.61, 125.35, 125.19, 123.92, 123.26, 122.84, 121.36, 120.32, 118.45, 113.26, 111.19, 110.02.

2.4.5 5-(2-(6-Bromo-9-(4-bromophenyl)-9*H*-carbazol-3-yl)vinyl)thiophene-2-carbaldehyde (**C5**)

$POCl_3$ (9 mL) was added into 60 mL of (DMF) dropwise at 0 °C under nitrogen atmosphere, and the mixture was warmed to room temperature. After stirring for 30 min, the solution of **C4** (2.55 g, 5 mmol) in 1,2-dichloroethane (10 mL) was added into the reaction in one portion. The reaction was heated to 60 °C and was stirred overnight. After cooling to room temperature, saturated sodium acetate aqueous solution was added. The mixture was extracted

with dichloromethane and the collected organic phases were dried over anhydrous $MgSO_4$. The solvent was removed on rotary evaporator and the residue was subjected to silica gel column and was eluted with petroleum ether/dichloromethane (1:2, *v*/*v*). The titled compound **C5** was obtained as an orange solid (2.15 g, 80% yield). ^{1}H NMR ($CDCl_3$, 300 Hz), δ (ppm): 9.83 (s, 1H), 8.21 (s, 1H), 8.12 (s, 1H), 7.74–7.71 (d, *J*=6.6 Hz, 2H), 7.64 (s, 1H), 7.57–7.54 (d, *J*=8.0 Hz, 1H), 7.49–7.47 (d, *J*=8.2 Hz, 1H), 7.38–7.35 (d, *J*=6.5 Hz, 2H), 7.25–7.18 (m, 4H), 7.13 (s, 1H). ^{13}C NMR ($CDCl_3$, 75 Hz), δ (ppm): 182.50, 152.60, 141.10, 139.77, 137.40, 135.90, 133.36, 129.26, 128.84, 128.48, 126.04, 125.80, 125.01, 123.30, 122.92, 121.63, 119.43, 119.13, 113.53, 111.33, 110.24.

2.4.6 Poly[2,7-(9,9-dioctylfluorene)-alt-6,4′-(5-(2-(9-phenyl-9*H*-carbazol-3-yl)vinyl)thiophene-2-carbaldehyde)] (PFC-CHO)

To a solution of 2,7-bis(4,4,5,5-tetramethyl-1,3,2-dioxaborolan-2-yl)-9,9-dioctylfluorene (321 mg, 0.5 mmol), **C5** (268 mg, 0.5 mmol) in 10 mL of degassed toluene, $Pd(PPh_3)_4$ (5 mg), sodium carbonate aqueous solution (2.0 M, 2 mL) and three drops of aliquat 336 was added into a 50 mL two-necked round-bottomed flask under nitrogen atmosphere. The reaction was heated to 95 °C and was stirred vigorously for 24 h. After cooling to room temperature, the mixture was precipitated from methanol. The collected polymer was dried and sequentially washed with acetone in a Soxhlet apparatus to remove oligomers and catalyst residues. The resulting material was dissolved in 15 mL of chloroform. The solution was filtered through a 0.45 μm PTFE filter, and precipitated from methanol to yield PFC-CHO as an orange solid (310 mg, 81% yield). ^{1}H NMR ($CDCl_3$, 300 Hz), δ (ppm): 9.88–9.78 (m, 1H), 8.50–24 (m, 2H), 7.98–7.93 (m, 2H), 7.92–7.88 (m, 2H), 7.84–7.63 (m, 8H), 7.60–7.31 (m, 4H), 7.20–7.12 (m, 2H), 2.16 (br, 4H), 1.28–1.14 (m, 24H), 0.88–0.79 (m, 6H). M_n=14.0 kg mol^{-1}, PDI=2.0.

2.4.7 Poly[2,7-(9,9-dioctylfluorene)-alt-6,4′-(2-((5-(2-(9-phenyl-9*H*-carbazol-3-yl)vinyl)thiophen-2-yl)methylene)-malononitrile)] (PFC-DCN)

To a solution of PFC-CHO (100 mg, 0.13 mmol) and malononitrile (300 mg, 4.5 mmol) in 10 mL of chloroform was added 0.5 mL of pyridine. The mixture solution was stirred in the dark for 24 h at room temperature, after which the resulting mixture was precipitated from methanol. The collected precipitate was dried and redissolved in 10 mL of chloroform. The solution was filtered through a 0.45 μm PTFE filter, and precipitated from methanol to yield PFC-DCN as a red solid (99 mg, 93% yield). ^{1}H NMR ($CDCl_3$, 300 Hz), δ (ppm): 8.50–8.26 (m, 2H), 8.00–7.82 (m, 4H), 7.74 (m, 7H), 7.67–7.48 (m, 6H), 7.46–7.31 (m, 1H), 7.22–7.19 (m, 1H), 2.17 (br, 4H), 1.30–1.14 (m, 24H), 0.88–0.79 (m, 6H). M_n=14.7 kg mol^{-1}, PDI=2.0.

2.4.8 Poly[2,7-(9,9-dioctylfluorene)-alt-6,4′-(1,3-diethyl-5-((5-(2-(9-phenyl-9*H*-carbazol-3-yl)vinyl)thiophen-2-yl)-methylene)2-thioxo-dihydropyrimidine-4,6(1H,5H)-dione)] (PFC-DTA)

To a solution of PFC-CHO (100 mg, 0.13 mmol) and 1,3-diethyl-2-thiobarbituric acid (500 mg, 2.5 mmol) in 10 mL of chloroform was added 0.5 mL of pyridine. The mixture solution was stirred in the dark for 24 h at room temperature, after which the resulting mixture was precipitated from methanol. The collected precipitate was dried and re-dissolved in 10 mL of chloroform. The solution was filtered through a 0.45 μm PTFE filter, and precipitated from methanol to yield PFC-DTA as red solid (117 mg, 95% yield). ^{1}H NMR ($CDCl_3$, 300 Hz), δ (ppm): 8.61 (s, 1H), 8.49–8.26 (m, 2H), 7.97–7.75 (m, 4H), 7.65–7.55 (m, 7H), 7.52–7.40 (m, 4H), 7.35–7.30 (m, 2H), 7.22–7.18 (m, 1H), 4.63 (br, 4H), 2.18 (br, 4H), 1.43–1.15 (m, 30H), 0.88–0.79 (m, 6H). M_n=13.5 kg mol^{-1}, PDI=1.6.

2.4.9 Poly[2,7-(*N*-9-heptadecanylcarbazole)-alt-6,4′-(5-(2-(9-phenyl-9*H*-carbazol-3-yl)vinyl)thiophene-2-carbaldehyde)] (PCC-CHO)

PCC-CHO was synthesized according to a procedure similar to that for PFC-CHO with corresponding monomers. ^{1}H NMR ($CDCl_3$, 300 Hz), δ (ppm): 9.88 (m, 1H), 8.54 (s, 1H), 8.41 (s, 1H), 8.27 (br, 2H), 8.01–7.86 (m, 4H), 7.77–7.58 (m, 8H), 7.48–7.31 (m, 2H), 7.20–7.18 (m, 2H), 4.81 (s, 1H), 2.50 (br, 2H), 2.09 (br, 2H), 1.34–1.19 (m, 24H), 0.89–0.79 (m, 6H). M_n=12.4 kg mol^{-1}, PDI=1.6

2.4.10 Poly[2,7-(*N*-9-heptadecanylcarbazole)-alt-6,4′-(2-((5-(2-(9-phenyl-9*H*-carbazol-3-yl)vinyl)thiophen-2-yl)-methylene)malononitrile)] (PCC-DCN)

PCC-DCN was synthesized according to a procedure similar to that for PFC-DCN. ^{1}H NMR ($CDCl_3$, 300 Hz), δ (ppm): 8.52–8.41 (m, 2H), 8.25 (br, 2H), 7.99–7.93 (m, 4H), 7.74 (s, 3H), 7.66–7.36 (m, 7H), 7.19 (2H), 4.79 (s, 1H), 2.49 (br, 2H), 2.07 (br, 2H), 1.43–1.18 (m, 24H), 0.88–0.80 (m, 6H). M_n=14.5 kg mol^{-1}, PDI=1.6.

2.4.11 Poly[2,7-(*N*-9-heptadecanylcarbazole)-alt-6,4′-(1,3-diethyl-5-((5-(2-(9-phenyl-9*H*-carbazol-3-yl)vinyl)thiophen-2-yl)methylene)2-thioxo-dihydropyrimidine-4,6-(1*H*,5*H*)-dione)] (PCC-DTA)

PCC-DTA was synthesized according to a procedure similar to that for PFC-DTA. ^{1}H NMR ($CDCl_3$, 300 Hz), δ (ppm): 8.60 (s, 1H), 8.50–8.41 (m, 2H), 8.29–8.25 (m, 3H), 7.97–7.78 (br, 3H), 7.80–7.77 (m, 4H), 7.64 (br, 4H), 7.56–7.49 (m, 4H), 7.39–7.29 (m, 2H), 4.79 (s, 1H), 4.62–4.57 (m, 4H), 2.48 (br, 2H), 2.07 (br, 2H), 1.43–1.18 (m, 30H), 0.88–0.80 (m, 6H). M_n=9.4 kg mol^{-1}, PDI=1.5.

3 Results and discussion

3.1 Molecules design, synthesis and characterization

The routes for the preparation of monomer **C5** and target conjugated polymers are depicted in Scheme 2. Compound **C1** was prepared from carbazole and 1,4-dibromobenzene via Ullmann reaction in DMPU with relative low yield due to the generation of bis-substituted byproduct. Vilsmeier-Haack formylation subsequently afforded compound **C2** from **C1**. Bromination of **C2** by bromine in dichloromethane yielded the dibromide compound **C3**, which was then reacted with diethyl (2-methylthiophene)-phosphonate to form compound **C4**. Aldehyde-functionalized dibromide monomer **C5** was finally obtained via Vilsmeier-Haack formylation. The two aldehyde-containing precursor polymers PFC-CHO and PCC-CHO were prepared by standard Suzuki polycondensation between the monomer **C5** with equimolar amount of fluorene-based diboronic ester and carbazole-based diboronic ester, respectively. The polymerization was performed in a biphasic system of toluene and 2.0 M aqueous Na_2CO_3 for 24 h. After purification, the two precursor polymers were obtained as orange solids and were applied for post-functionalization. The target polymers PFC-DCN, PFC-DTA, PCC-DCN, PCC-DTA were obtained by treating PFC-CHO or PCC-DTA with malononitrile or 1,3-diethylbarbituric acid, respectively, through pyridine-catalyzed Knoevenagel condensation. All four target polymers showed good solubility in common organic solvents such as chloroform and chlorobenzene at room temperature. The molecular weight and molecular weight distribution of the polymers were estimated by gel permeation chromatography (GPC) using THF as an eluent calibrated with a series of monodispersed polystyrene standards. The number-average molecular weight (M_n) of PFC-DCN, PFC-DTA, PCC-DCN, and PCC-DTA were estimated to be 14.7, 13.5, 14.5 and 9.7 kg mol^{-1} with PDI of 2.0, 1.6, 1.6, and 1.5, respectively.

3.2 Thermal properties

Thermal behavior of the resulting polymers was evaluated by differential scanning chromatography (DSC) and thermogravimetric analysis (TGA) under nitrogen atmosphere, and the results are shown in Figure 1 and Table 1. As illustrated in Figure 1(a), the polymers exhibit good thermal stability in the temperature range from 40 to 800 °C in the nitrogen atmosphere. The 5%-weight loss temperatures (T_ds) are 386, 315, 386 and 315 °C for PFC-DCN, PFC-DTA, PCC-DCN, and PCC-DTA respectively. DSC

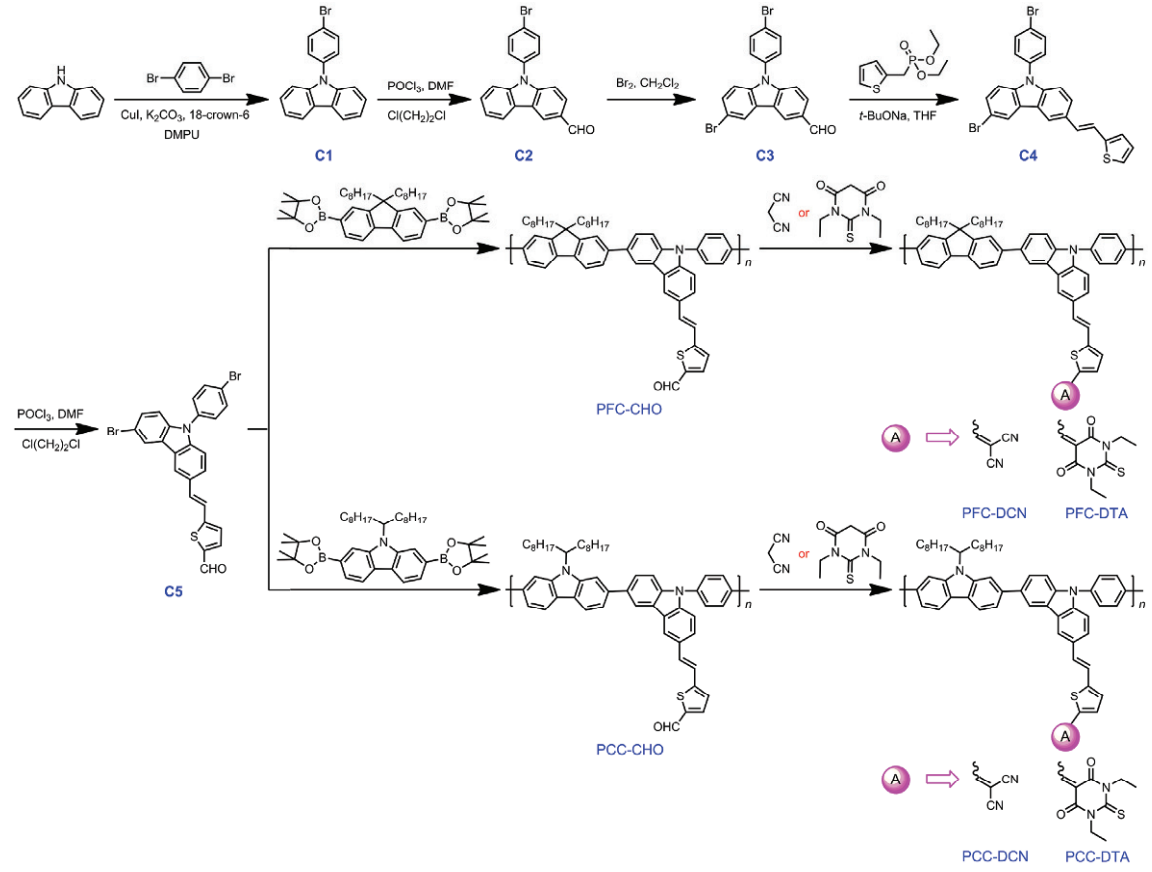

Scheme 2 The routes for the preparation of new monomers and target conjugated polymers (color online).

Table 1 Reaction yields, molecular weights and thermal properties of PFC-DCN, PFC-DTA, PCC-DCN, and PCC-DTA

Polymer	Yield (%)	M_n (kg mol^{-1})	PDI	T_d (°C)
PFC-DCN	93	14.7	2.0	386
PFC-DTA	95	13.5	1.6	315
PCC-DCN	92	14.5	1.6	386
PCC-DTA	93	9.7	1.5	315

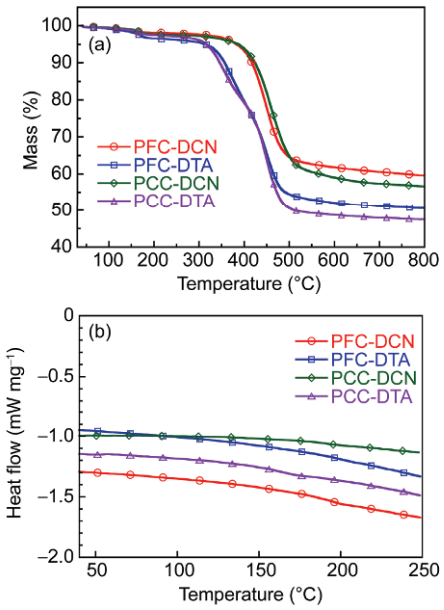

Figure 1 TGA (a) and DSC (b) plots of PFC-DCN, PFC-DTA, PCC-DCN and PCC-DTA.

measurements show that there is no distinct exothermal transition for these copolymers in the second heating cycle over the temperature range of 40–250 °C (Figure 1(b)), indicating that no crystalline behavior or phase transition happens in this temperature range.

3.3 Optical properties

The UV-Vis absorption spectra of the resulting polymers in dilute solutions and in films are demonstrated in Figure 2(a) and 2(b), respectively. Relevant parameters are summarized in Table 2. The polymers show two resemble absorption bands, where the first absorption peak below 400 nm can be attributed to the characteristic absorbance of π-π* transition of polymer backbones, while the low-energy absorbance, located in the region of 400–700 nm, can be attributed to the intramolecular charge transfer (ICT) effects between the electron-donating carbazole moieties in main chain and electron-withdrawing side-chains. Along with the increase of electron-withdrawing ability of the pendant acceptors, the ICT absorption peak significantly red-shifted from around 500 nm for malononitrile-attached polymers (PFC-DCN and PCC-DCN) to around 550 nm for 1,3-diethyl-2-thiobarbituric acid-attached polymers (PFC-DTA and PCC-DTA). It is worth mentioning that the same acceptor side chain results in similar ICT absorption peak in spite of the different conjugated main chains. In high energy region, these copolymers also show a very close absorption peak, indicating similar conjugation length along the main chains. The absorption onset in thin films is 574, 631, 576, and 631 nm for PFC-DCN, PFC-DTA, PCC-DCN, and PCC-DTA, respectively. The optical band gaps (E_g) are calculated to be 2.16 eV for PFC-DCN, 1.96 eV for PFC-DTA, 2.15 eV for PCC-DTA, and 1.96 eV for PCC-DTA. These results clearly suggest that the optical properties of the resulting polymers can be readily tuned by changing pendant acceptors.

3.4 Electrochemical properties

The electronic structures of the copolymers were investigated by cyclic voltammetry (CV) experiments. The ferrocene/ferrocenium (Fc/Fc^+) reference was employed as an internal standard, which was supposed an absolute energy of –4.8 eV vs. vacuum level [42]. Under the same experimental conditions, the oxidation potential of Fc/Fc^+ was measured to be 0.31 V with respect to the SCE reference electrode. Highest occupied molecular orbital (HOMO) energy levels are estimated to be –5.50 eV for PFC-DCN,

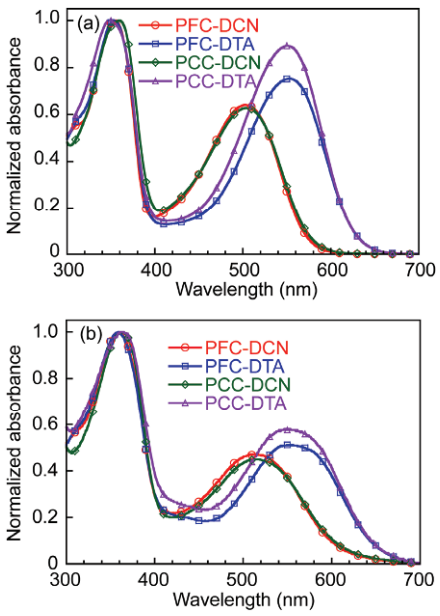

Figure 2 UV-Vis absorption spectra of PFC-DCN, PFC-DTA, PCC-DCN and PCC-DTA in chloroform solutions (a) and in films (b).

Table 2 Optical and electrochemical properties of PFC-DCN, PFC-DTA, PCC-DCN and PCC-DTA

Polymers	λ_{abs} [a] (nm)	λ_{abs} [b] (nm)	E_{gap} [c] (eV)	E_{ox} (V)	HOMO (eV)	LUMO (eV)
PFC-DCN	353, 502	361, 511	2.16	1.12	–5.50	–3.34
PFC-DTA	354, 553	359, 558	1.96	1.19	–5.50	–3.54
PCC-DCN	357, 503	359, 516	2.15	1.02	–5.49	–3.34
PCC-DTA	348, 550	362, 553	1.96	1.14	–5.50	–3.54

a) In solution; b) in film; c) calculated from the absorption onset in film

–5.50 eV for PFC-DTA, –5.49 eV for PCC-DCN, and –5.50 eV for PCC-DTA (Table 2). Since no reliable reduction characteristics were recorded in our measurements, the lowest unoccupied molecular orbital (LUMO) energy levels are calculated from HOMO levels and optical band gaps. As listed in Table 2, PFC-DCN, PFC-DTA, PCC-DCN, and PCC-DTA show a LUMO level of –3.34, –3.54, –3.34, and –3.54 eV, respectively.

It is worth noting that the HOMO levels of these copolymers show no obvious disparity despite the presence of different acceptors in side chains. As shown in Figure 3(b), the LUMO-LUMO offset, and HOMO-HOMO offset between the polymers and $PC_{71}BM$ are all larger than 0.3 eV, providing sufficient driving forces for efficient electron transfer [43] and hole transfer [44]. Moreover, the deep-lying HOMO levels of the polymers are appreciated for getting high open circuit voltage (V_{oc}) in solar cells, as V_{oc} is related to the offset between the HOMO levels of donor and the LUMO levels of acceptor [45].

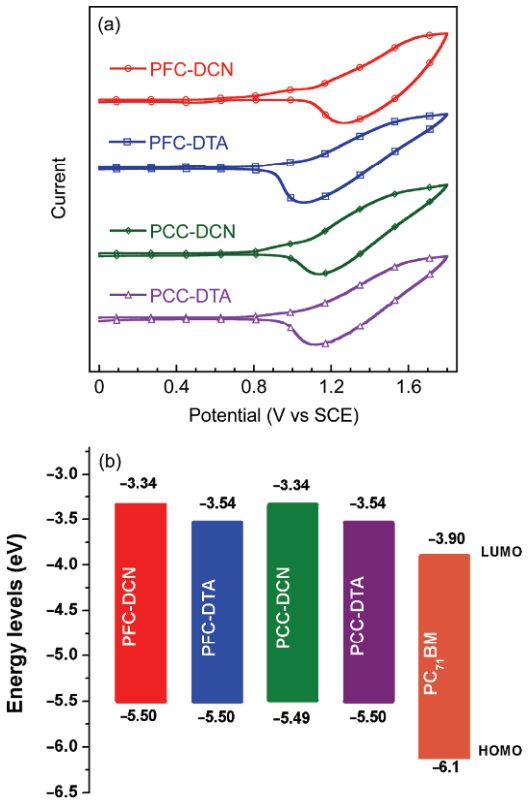

Figure 3 (a) Cyclic voltammograms curves of the polymers films measured in 0.1 M Bu_4NPF_6 vs. SCE in acetonitrile; (b) energy levels of polymers and $PC_{71}BM$ (color online).

3.5 Photovoltaic properties

The photovoltaic properties of the resulting copolymers are evaluated in device with a structure of ITO/ PEDOT:PSS (40 nm)/active layer (80–90 nm)/Ca (5 nm)/Al (100 nm), wherein the photoactive layer uses $PC_{71}BM$ as the acceptor with the optimized weight ratio of copolymer:$PC_{71}BM$ of 1:4. The *J*-*V* characteristics of the solar cells are shown in Figure 4(a), and relevant photovoltaic parameters are summarized in Table 3. PCC-DCN shows the best photovoltaic performance among all the polymers with a V_{oc} of 0.80 V, a short-circuit current density (J_{sc}) of 4.42 mA cm^{-2}, a fill factor (FF) of 0.39, and a PCE of 2.0%. All PSCs exhibited the same V_{oc}, which is consistent with the HOMO level of the polymers. The PCEs of these devices are limited by J_{sc} and FF. The J_{sc} is lower than 4 mA cm^{-2}, while FF is lower than 0.40 for all polymers. To confirm the photo-response and J_{sc} of the bulk-heterojunction (BHJ) solar cells based on

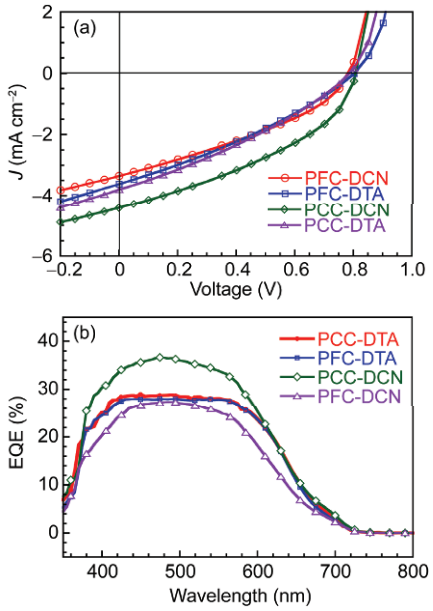

Figure 4 The *J*-*V* characteristics (a) and EQE spectra (b) of the devices with the configuration of ITO/PEDOT:PSS (40 nm)/active layer (80–90 nm)/Ca (5 nm)/Al (100 nm) (color online).

Table 3 Photovoltaic parameters of the BHJ-PSCs with the device configuration of ITO/PEDOT:PSS/polymer:$PC_{71}BM$ (1:4)/Ca/Al under the illumination of simulated AM 1.5G conditions (100 mW cm^{-2}) and hole mobility of the neat polymers and polymer:$PC_{71}BM$ (1:4) blends estimated by SCLC method

Polymer	V_{oc} (V)	J_{sc} (mA cm^{-2})	FF	PCE (%)	$\mu_{polymer}$(cm^2 V^{-1} s^{-1})	μ_{blend} (cm^2 V^{-1} s^{-1})
PFC-DCN	0.80	3.4	0.35	1.3 (1.3)	1.2×10^{-4}	5.6×10^{-4}
PFC-DTA	0.80	3.6	0.31	1.3 (1.1)	6.0×10^{-4}	6.2×10^{-4}
PCC-DCN	0.80	4.4	0.39	2.0 (2.0)	3.9×10^{-4}	5.0×10^{-4}
PCC-DTA	0.80	3.8	0.31	1.4 (1.3)	1.5×10^{-4}	1.8×10^{-4}

the resulting polymers, the external quantum efficiency (EQE) of devices illuminated by monochromatic light were determined. As presented in Figure 4(b), solar cell of PCC-DCN demonstrates the most efficient photo-response with relative high EQE over 30% in a broad range from 400 to 600 nm, while the other polymers produce EQE lower than 30%. The low J_{sc} and FF may be attributable to the amorphous nature of the polymers, as evidenced by the DSC studies. Generally, the amorphous films result in poor charge transport abilities intrinsically and suboptimal BHJ morphologies lacking pure polymer domains. As a result, the sweep out of charge carriers in such well-mixed polymer:fullerene blend films is inefficient, which thereby leads to low J_{sc} and FF [46,47].

3.6 Hole mobility

Since charge transport capacity is one of key factors determining device performance, it is of vital importance to get insight into the hole mobility of the devices. Hole-only devices with a configuration of ITO/PEDOT:PSS/active layer/MoO_3/Al were fabricated. Hole mobilities are estimated by using space charge limited current (SCLC) method, which can most accurately evaluate the charge transport ability of the BHJ solar cells active layer [48,49]. The $J^{1/2}$-V plots of the devices are shown in Figure 5. The mobility values of the polymers and blends are summarized in Table 3. The hole mobilities are 1.2×10^{-4}, 6.0×10^{-4}, 3.9×10^{-4}, and 1.5×10^{-4} cm^2 V^{-1} s^{-1}, respectively, for the neat polymer films of PFCDCN, PFCDTA, PCCDCN, and PCCDTA. The hole mobilities of the corresponding polymer:$PC_{71}BM$ blends are 5.6×10^{-4}, 6.2×10^{-4}, 5.0×10^{-4} and 1.8×10^{-4} cm^2 V^{-1} s^{-1}, respectively. The state-of-the-art photovoltaic polymers in blend films usually exhibit SCLC hole mobilities of 10^{-3} cm^2 V^{-1} s^{-1}, a value that is well recognized for achieving balanced charge transport in BHJ films and high FF [50]. The relative low hole mobilities of the acceptor-pended polymers described in this paper are thus, at least partially, responsible for the low J_{sc} and FF of the resulting BHJ solar cells.

3.7 Blend morphology

The film morphology of the photoactive layer is essential to the performance of PSCs [7]. Thus the surface topography

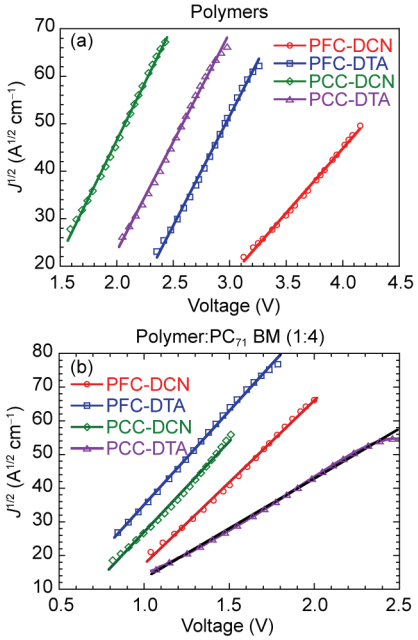

Figure 5 $J^{1/2}$-V characteristics of hole-only diodes with a configuration of ITO/PEDOT:PSS/active layer/MoO_3/Al for neat polymer films (a) and polymer:$PC_{71}BM$ blend films (b). The solid lines denote the fitting curves (color online).

of the polymer:$PC_{71}BM$ BHJ films was investigated by tapping mode atomic force microscopy (AFM). The relevant images are shown in Figure 6. The films were prepared on top of the ITO/PEDOT:PSS layer with the same procedures as those for the fabrication of solar cell devices. As shown in Figure 5, one can observe the pronounced variation of films morphology of the copolymer:$PC_{71}BM$ blends, the PCC-DCN based blend film shows smooth surface with root-mean-square (RMS) roughness of 0.496 nm, indicating the uniform mixing of PCC-DCN and $PC_{71}BM$. The surface of PCC-DTA:$PC_{71}BM$ film is slightly rougher with an RMS roughness of 0.565 nm along with the emergence of aggregates, mainly owing to the worse solubility of PCC-DTA in processing solvents. The blend films of fluorene-based polymers exhibit distinct phase separation with large domain size, leading to rather coarse surfaces with RMS roughness of 1.187 nm for PFC-DCN, and 4.327 nm for PFC-DTA, respectively. The larger domains observed in fluorene-based polymer films are attributable to their relative low solubilities in processing solvents.

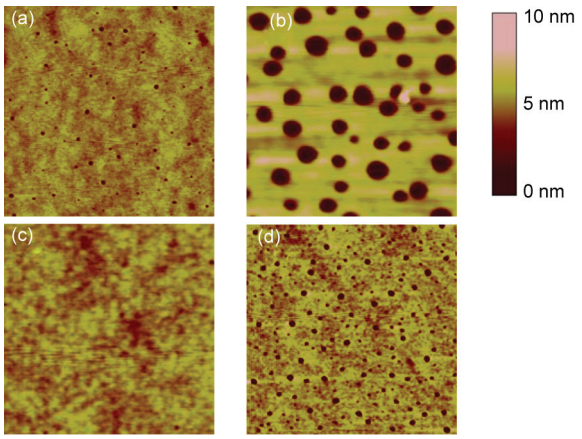

Figure 6 AFM height images of polymer:$PC_{71}BM$ (1:4, wt/wt) blend films with size of 5 μm×5 μm for PFC-DCN:$PC_{71}BM$ (a), PFC-DTA:$PC_{71}BM$ (b), PCC-DCN:$PC_{71}BM$ (c), and PCC-DTA:$PC_{71}BM$ (d) (color online).

4 Conclusions

In summary, we developed a series of new acceptor-pended conjugated polymers (PFC-DCN, PFC-DTA, PCC-DCN, and PCC-DTA), which feature a novel carbazole-derived building unit for polymer solar cells. The resulting polymers were fully characterized by TGA, DSC, UV-Vis, and CV. All the resulting polymers exhibited good solubility, excellent thermal stability, and deep-lying HOMO energy levels. The absorption spectra and energy levels of these polymers could be readily tuned by altering the pendant acceptor groups. The photovoltaic properties of the resulting polymers were studied by blending the polymers with $PC_{71}BM$. All devices exhibited moderate performances with the highest PCE of 2.0%. The relative low PCEs of the PSCs are mainly attributable to the low hole mobilities of the polymers. These observations indicate that the further development of photovoltaic polymers based on the acceptor-pended design should focus on improving charge transport abilities, besides the manipulation of electronic structures.

Acknowledgments This work was supported by the Ministry of Science and Technology (2014CB643501), the National Natural Science Foundation of China (21520102006, 21490573, 51361165301) and the Guangdong Natural Science Foundation (S2012030006232).

Conflict of interest The authors declare that they have no conflict of interest.

1 Beaujuge PM, Fréchet JMJ. *J Am Chem Soc*, 2011, 133: 20009–20029
2 Li YF. *Acc Chem Res*, 2012, 45: 723–733
3 Li G, Zhu R, Yang Y. *Nat Photonic*, 2012, 6: 153–161
4 Dou LT, You JB, Hong ZR, Xu Z, Li G, Street RA, Yang Y. *Adv Mater*, 2013, 25: 6642–6671
5 Heeger AJ. *Adv Mater*, 2014, 26: 10–28
6 Lu LY, Zheng TY, Wu QH, Schneider AM, Zhao DL, Yu LP. *Chem Rev*, 2015, 115: 12666–12731
7 Liu YH, Zhao JB, Li ZK, Mu C, Ma W, Hu HW, Jiang K, Lin HR, Ade H, Yan H. *Nat Commun*, 2014, 5: 5293
8 Liao SH, Jhuo HJ, Yeh PN, Cheng YS, Li YL, Lee YH, Sharma S, Chen SA. *Sci Rep*, 2014, 4: 6813
9 Zhang SQ, Ye L, Zhao WC, Yang B, Wang Q, Hou JH. *Sci China Chem*, 2014, 58: 248–256
10 Vohra V, Kawashima K, Kakara T, Koganezawa T, Osaka I, Takimiya K, Murata H. *Nat Photonic*, 2015, 9: 403–408
11 Wu ZH, Sun C, Dong S, Jiang XF, Wu SP, Wu HB, Yip HL, Huang F, Cao Y. *J Am Chem Soc*, 2016, 138: 2004–2013
12 He ZC, Xiao B, Liu F, Wu HB, Yang YL, Xiao S, Wang C, Russel T P, Cao Y. *Nat Photonic*, 2015, 9: 174–179
13 Chen JD, Cui CH, Li YQ, Zhou L, Ou QD, Li C, Li YF, Tang JX. *Adv Mater*, 2015, 27: 1035–1041
14 Zhao JB, Li YK, Yang GF, Jiang K, Lin HR, Ade H, Ma W, Yan H. *Nat Energy*, 2016, 1: 15027
15 Zhou HX, Yang LQ, You W. *Macromolecules*, 2012, 45: 607–632
16 Li WW, Roelofs WS, Turbiez M, Wienk MM, Janssen RA. *Adv Mater*, 2014, 26: 3304–3309
17 Li WW, Hendriks KH, Furlan A, Wienk MM, Janssen RA. *J Am Chem Soc*, 2015, 137: 2231–2234
18 Duan CH, Furlan A, van Franeker JJ, Willems RE, Wienk MM, Janssen RA. *Adv Mater*, 2015, 27: 4461–4468
19 Zhang ZG, Li YF. *Sci China Chem*, 2015, 58: 192–209
20 Liu C, Wang K, Gong X, Heeger AJ. *Chem Soc Rev*, 2016, 45: 4825–4846
21 Duan CH, Huang F, Cao Y. *J Mater Chem*, 2012, 22: 10416–10434
22 Huang F, Chen KS, Yip HL, Hau SK, Acton O, Zhang Y, Luo JD, KY Jen A. *J Am Chem Soc*, 2009, 131: 13886–13887
23 Duan CH, Chen KS, Huang F, Yip HL, Liu SJ, Zhang J, KY Jen A, Cao Y. *Chem Mater*, 2010, 22: 6444–6452
24 Duan CH, Cai WZ, Huang F, Zhang J, Wang M, Yang TB, Zhong CM, Gong X, Cao Y. *Macromolecules*, 2010, 43: 5262–5268
25 Duan CH, Wang CD, Liu SJ, Huang F, Choy C W, Cao Y. *Sci China Chem*, 2011, 54: 685–694
26 Li W, Li QD, Liu SJ, Duan CH, Ying L, Huang F, Cao Y. *Sci China Chem*, 2015, 58: 257–266
27 Zhang ZG, Liu YL, Yang Y, Hou KY, Peng B, Zhao GJ, Zhang MJ, Guo X, Kang ET, Li YF. *Macromolecules*, 2010, 43: 9376–9383
28 Li S, He ZC, Zhong AS, Yu J, Wu HB, Zhou Y, Chen SA, Zhong C, Qin JG, Li Z. *Polymer*, 2011, 52: 5302–5311
29 Fan HJ, Zhang ZG, Li YF, Zhan XW. *J Polym Sci Part A*: *Polym Chem*, 2011, 49: 1462–1470
30 Chen DG, Yang Y, Zhong C, Yi ZR, Wu F, Qu L, Li YF, Qin JG. *J. Polym Sci Part A*: *Polym Chem*, 2011, 49: 3852–3862
31 Zeigler DF, Chen KS, Yip HL, Zhang Y, Jen AKY. *J Polym Sci Part A*: *Polym Chem*, 2012, 50: 1362–1373
32 Xie HM, Zhang K, Duan CH, Liu SJ, Huang F, Cao Y. *Polymer*, 2012, 53: 5675–5683
33 Li HH, Luo H, Cao ZC, Gu ZJ, Shen P, Zhao B, Chen HJ, Yu G, Tan ST. *J Mater Chem*, 2012, 22: 22913–22921

34 Liao LY, Zhang W, Xiao Z, Cao JM, Liu ZP, Zuo QJ, Ding LM. *Polym J*, 2013, 45: 571–575
35 Chen YC, Hsu CY, Ho CY, Tao YT, Lin JT. *Org Electron*, 2013, 14: 2290–2298
36 Mei SL, Wu F, Huang YS, Zhao B, Tan ST. *Eur Polym J*, 2015, 67: 31–39
37 Xu XP, Feng K, Li K, Peng Q. *J Mater Chem A*, 2015, 3: 23149–23161
38 Li Y, Xu XP, Li ZJ, Yu T, Peng Q. *Sci China Chem*, 2015, 58: 276–285
39 Liu YR, Chan LH, Tang HY. *J Polym Sci Part A*: *Polym Chem*, 2015, 53: 2878–2889
40 Ranger M, Rondeau D, Leclerc M. *Macromolecules*, 1997, 30: 7686–7691
41 Blouin N, Michaud A, Leclerc M. *Adv Mater*, 2007, 19: 2295–2300
42 Pavlishchuk VV, Addison AW. *Inorg Chim Acta*, 2000, 298: 97–102
43 Dennler G, Scharber MC, Brabec CJ. *Adv Mater*, 2009, 21: 1323–1338
44 Ren GQ, Schlenker CW, Ahmed E, Subramaniyan S, Olthof S, Kahn A, Ginger DS, Jenekhe SA. *Adv Funct Mater*, 2013, 23: 1238–1249
45 Brabec CJ, Cravino A, Meissner D, Sariciftci NS, Fromherz T, Rispens MT, Sanchez L, Hummelen JC. *Adv Funct Mater*, 2001, 11: 374–380
46 Hedley GJ, Ward AJ, Alekseev A, Howells CT, Martins ER, Serrano LA, Cooke G, Ruseckas A, Samul IDW. *Nat Commun*, 2013, 4: 2867
47 Huang Y, Kramer EJ, Heeger AJ, Bazan GC. *Chem Rev*, 2014, 114: 7006–7043
48 Mihailetchi V, Wildeman J, Blom P. *Phys Rev Lett*, 2005, 94: 126602
49 Yao Y, Shi CJ, Li G, Shrotriya V, Pei QB, Yang Y. *Appl Phys Lett*, 2006, 89: 153507
50 Duan CH, Huang F, Cao Y. *Polym Chem*, 2015, 6: 8081–8098